Dynamic hip fracture modelling

John Arundell[1] Aaron Blicblau[2] David Richards[3]
Manmohan Singh[4]

(Received 13 August 2008; revised 15 October 2008)

Abstract

A treatment of neck of femur fractures is internal fixation using a dynamic hip screw. This article investigates the effect of the angle of such a dynamic hip screw on the stresses developed under loading in a human femur. The modelling is informed by an examination of Medicare Australia data which indicates that women aged 65 years or over are the primary recipients of an internal fixation of the neck of femur. Development of a series of finite element models with incremental changes in angle allows determination of the stresses developed in use. Regression analysis of the data obtained from the finite element analysis reveals a strong negative association between angle and stress. The results obtained will assist in the selection of dynamic hip screw angles appropriate for individual patients.

http://anziamj.austms.org.au/ojs/index.php/ANZIAMJ/article/view/1434 gives this article, © Austral. Mathematical Soc. 2008. Published November 6, 2008. ISSN 1446-8735. (Print two pages per sheet of paper.)

Contents

1 Introduction **C221**

2 Dynamic hip screw mounted in an approximated bone **C224**
2.1 The bone assembly C225
2.2 Loading conditions C228

3 Statistical analysis **C230**
3.1 Linear regression C232

4 Conclusion **C234**

References **C234**

1 Introduction

A fracture of the proximal human femur is more commonly known as a hip fracture. Neck of femur (NOF) fractures account for over a third of all hip fractures (Johansson et al. [4]). The neck is the weakest part of the femur and the bone carries tremendous stresses (Marieb [6]). There are two operative solutions to hip fracture: total hip replacement (THR); and internal fixation (IF). THR requires the surgical removal of the femoral neck, head and some of the surrounding bone to accommodate a replacement prosthesis. Typically this prosthesis is anchored by press fitting a long blade-like part into an appropriately sized hole in the femur. Once the operation is complete, the prosthesis takes on the role of support that the original bone once fulfilled, as shown in Figure 1 (Weinrauch [12]). The aim of IF is to preserve the original bone by mechanically stabilising the fracture so that bone healing may begin. The device used either consists of screws or is affixed to the bone by them. An X-ray image of a dynamic hip screw (DHS) and IF are shown in Figure 2 [3].

FIGURE 1: X-ray of total hip replacement.

FIGURE 2: X-ray of internal fixation and dynamic hip screw.

IF is a less invasive and quicker procedure than THR. Kemler et al. [5] report that the generally accepted failure, or revision surgery, rate of IF is 15%. It is desirable to minimise this rate. Edwards et al. [2] succeeded in developing an intra-operative test to determine whether the screws in an IF would fail under predicted normal loading conditions. Although targeted at failure of the screws in an IF, rather than the IF itself, the study still looks at ways to improve upon the failure rate of IF in general. A limitation of the study is that only one NOF angle, 135°, is considered. The angle of 135° is that of the pin and plate IF, corresponding to a NOF angle of approximately 135°. In practice, NOF angles vary quite widely. For example, in the Omega-3 brochure (Stryker [10]) compression hip screw IFs compatible with NOF angles from 130° to 150° are listed. According to Nissen et al. [8] the standard deviation of the NOF angle is 5° for both sexes, with means 131° for men and 129° for women.

To inform the subsequent analysis, relevant Australian data on hip fracture procedures are examined (Medicare Australia [7]) . The frequencies of IF of the NOF procedures largely increase with age. About 71% of the procedures are conducted on females aged 65 or above. If male patients in this age group are included, the overall percentage of IF of the NOF procedures accounted for increases to 90% (Medicare Australia [7]).

This article investigates the relationship between the stress placed on an IF and angle of NOF.

2 Dynamic hip screw mounted in an approximated bone

We now make computer models of the dynamic hip screw (DHS) for different NOF angles and use them to perform finite element analysis (FEA) of the loads on the DHS. The angle referred to here is that which the barrel of the

DHS makes with its body, corresponding to the angle that the femur makes with its neck (see Figure 2). We model the DHS being placed under loads typically experienced when an individual stands up placing full weight on the leg, and record the resulting stresses. Initially, we aim to model each part of the DHS independently and also obtain an approximate model for the proximal femur. The parts of the DHS are then put together in an assembly and analysed using FEA.

A lag screw and compression plate model of IF was selected for experimentation and a model of this assembled IF was developed in Solidworks [9]. Cosmosworks [1] was then used to automatically generate a Finite Element Model (FEM). Once the FEM was developed a series of boundary conditions were entered to correspond to approximate loading conditions from the target population. Once the Solidworks [9] model, FEM and loading conditions are developed, an FEA can be performed in Cosmosworks [1] for stress. This would locate highly stressed regions and potentially areas of failure. Then the process of FEA is performed again, with the IF angle varying from 115° to 150° and with similar loading conditions. The variation of the IF angle is taken to exceed three standards of deviation from the mean of the target population or it risks becoming statistically insignificant. The results of the FEA were tested against the results of physical experiments targeted to areas of interest revealed in the FEA. The total number of nodes considered ranged between eighty to ninety thousand depending on the specific FEM.

2.1 The bone assembly

The best way to model the bone is as an assembly of

- the head of the femur with part of the femoral neck attached,
- the body of the femur with the rest of the femoral neck, and
- a small disc to sit between them at the width of the femoral neck.

TABLE 1: Bone dimensions used in FEA modelling (in mm).

	Hip axis length	Neck width	Femoral head radius
Nissen et al. model μ± SD	95 ± 6	33 ± 3	23 ± 2
Present Model	112	33	23

Including the disc allows different properties to be given to the fracture site compared to other parts of the bone. We thus potentially represent the amount of bone healing that has occurred. Young's moduli, Poisson's ratios and moduli of rigidity have been used to represent the mechanical properties of bone through various stages of healing. The dimensions of the bone, other than the angle of the femoral neck, are taken from the article by Nissen et al. [8], and are based on the mean values given for women in the study, as summarised in Table 1.

According to Synthes [11], the hip axis length value used is the minimum value that prevents the head being drilled through, which could potentially weaken the structure. One problem with the modelling of the bone is that the reverse impression of the lag screw's thread is exceedingly difficult to represent. To solve this problem, the part of the hole that housed the screw thread is made wide enough not to interfere with the extremities of the DHS screw thread. Additionally, the part of the hole that just houses the shaft of the screw is made to be flush with the shaft of the screw.

The DHS itself is made up of three kinds of parts, namely the plate, lag screw and bone screw. In the final assembly there is one each of the plate and lag screw, but six of the bone screws. Most of the dimensions of these model parts in the DHS are based on approximate comparative dimensions taken from images given by Stryker [10] and Synthes [11]. The bone screws, very standard parts, are approximated as simple cylinders without compromising the FEA. The lag screw, on the other hand, is seen as a critical part as it transmits a large proportion of the body weight to the rest of the DHS. Since

TABLE 2: Axial (P_a) and tangential loads (P_p) on the lag screw in Pascals.

Angle(°)	115	117.5	120	122.5	125
P_a	1.14E+07	1.25E+07	1.35E+07	1.45E+07	1.55E+07
P_p	8.66E+05	8.47E+05	8.27E+05	8.06E+05	7.83E+05
Angle(°)	127.5	130	132.5	135	137.5
P_a	1.64E+07	1.73E+07	1.82E+07	1.91E+07	1.99E+07
P_p	7.58E+05	7.32E+05	7.04E+05	6.76E+05	6.45E+05
Angle(°)	140	142.5	145	147.5	150
P_a	2.07E+07	2.14E+07	2.21E+07	2.27E+07	2.34E+07
P_p	6.14E+05	5.82E+05	5.48E+05	5.13E+05	4.78E+05

it is perceived to be an important component in the bearing and transmission of load, the description of the screw thread by Synthes [11] is modelled as closely as possible.

In order to simplify the modelling, an approximate femur in the analysis is abandoned and the DHS is remodelled as a single part. Since the single part model is not incorporated into a larger 'bone and DHS assembly' there is no requirement that the lag screw be of a minimum length. As such, the length of the lag screw in the single part model is reduced from that of the assembly of parts model. It is reduced to be closer to the mean hip axis length as determined by Nissen et al. [8].

Angles between 114° and 144° are within three standard deviations of the female population mean found by Nissen et al. [8]. The product literature from Stryker [10] and Synthes [11] reveals that the ranges on offer from these commercial suppliers are 130° to 150° (in 5° increments) and 135° to 150° (in 5° increments) respectively. Therefore the range modelled is from 115° to 150°, in increments of 2.5°. Finite element models (FEM) are generated for each angle. Results from the FEA for axial and tangential loads on the lag screw are given in Table 2.

2.2 Loading conditions

We assume that the entire weight of the person is transmitted through the head section of the broken femur to the DHS. This loading is approximated as a pair of perpendicular uniformly distributed loads, one acting axially along and at the femoral head end of the lag screw (P_a), the other parallel to the face of the barrel of the compression plate and the length of the compression plate, acting on the surface of the lag screw's shaft at the femoral head end (P_p). In our model as shown in Figure 3, the non-scaled vector representations of the restraints are in green and the loads in red. The green arrows indicate that the given surface is incapable of moving in the indicated direction.

The entities completely constrained are shown in Figure 3. These are the cylindrical surfaces and the bottoms of each of the bone screws. There is a special constraint applied to the barrel of the compression plate to represent that this part is anchored in solid bone away from the site of the fracture. The barrel is constrained so that it cannot change its angle with the rest of the compression plate: it cannot act as a hinge, nor bend at its corner. The rest of the DHS is unconstrained.

The length of the lag screw shaft that the load P_p acts on is chosen to be $\approx 28.5\,\mathrm{mm}$, about halfway between the end of the compression plate's barrel and the lag screw's end. In reality, this length would depend on where the fracture occurs in the patient and so a reasonably general area, the middle, is chosen to be the site of the fracture.

The loads are developed for a person weighing 62 kilograms standing with full weight on one leg. The weight of 62 kilograms is chosen as it is the mean of the female sample used by Nissen et al. [8]. Under this model, such a person's full weight would be borne by the DHS and none by the partially healed bone. While not the recommended loading situation for a DHS in practice, it is representative of a worst case, or emergency scenario. In order to properly define the loading conditions, certain reference geometries are

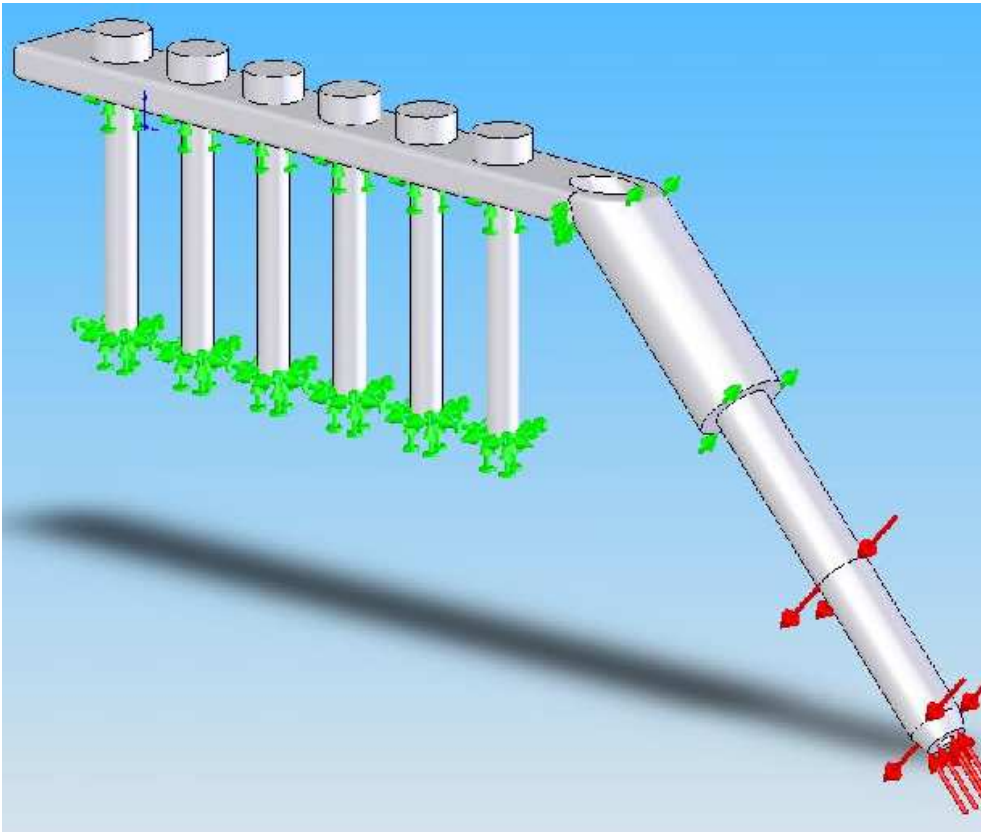

FIGURE 3: DHS loading conditions for our actual model.

incorporated. To save weight in the DHS, a 0.1 mm reduction in lag screw diameter is introduced. FEA results show that the average size of the cells in the mesh is 2.3 mm^3 (1.3 mm to a side for cubes) and the overall diameter is 8 mm at that point. These values give an approximate change of 1.3% in the diameter globally and 3.8% in the width of the cells at the surface. A notch is found to develop in the FEM model (as a result of the Solidworks/ Cosmosworks modelling) when rounded edges are kept in all models where the angle of the compression plate is less than 135°. We refined the mesh until an accuracy of three significant figures was achieved.

3 Statistical analysis

The major outcome of each of the FEM is a list of values for Von Mises stress at each of the node points. To make use of these figures the list of stresses and their nodes for each different angle of DHS are sorted in order of descending stress magnitude. To minimise the effect of outliers on the overall analyses and conclusions the 95th percentile stress, not the maximum stress, is used.

The base family is the family with a notched compression plate development for models with an angle less than 135°. There is an approximate 37% reduction in the stress experienced from the 115° angle to the 150° angle for this family. While this might seem to be a conclusive indication that an increase in angle decreases the stress in the DHS over the given range, such results or their scale might well be due to the errors inherent in the experimental process. There appears to be a negative linear relationship between the Von Mises stress and the angle of the compression plate.

Figure 4 shows that the base family of models, with notch development for angles less than 135°, is slightly more stressed than the alternate (divergent) model family (unnotched). The models with no notch but sharper edges lead to a smaller magnitude of Von Mises stress. At all data points the unnotched family has less stress than the base family with notch development, despite

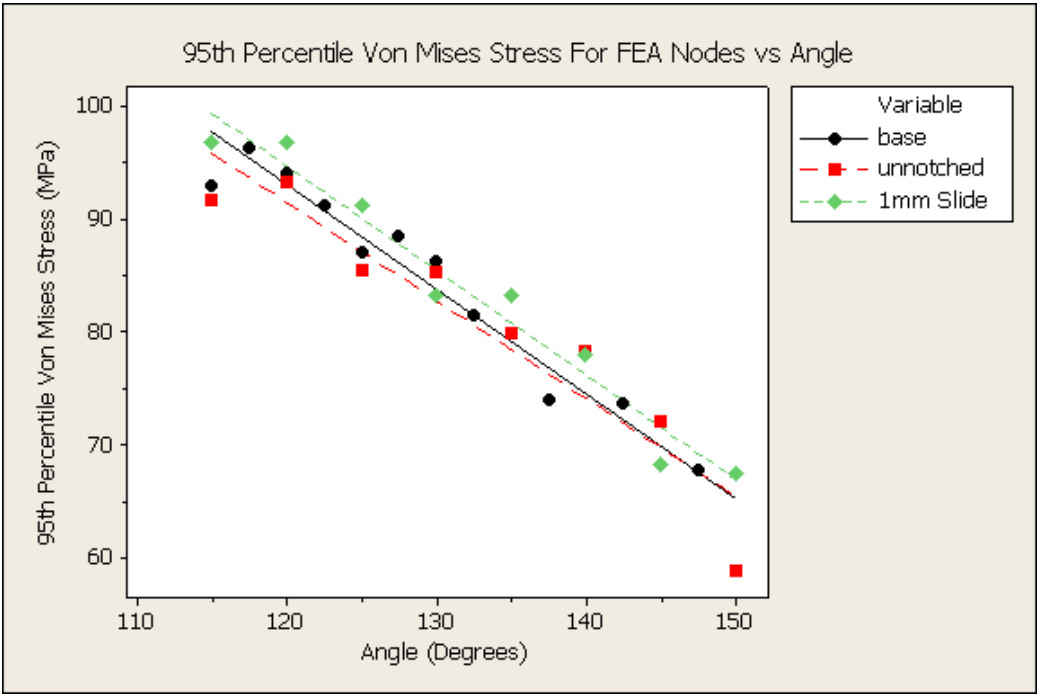

FIGURE 4: 95th percentile stresses for all families of models.

TABLE 3: Summary of regression results by model family.

	r	b_0	b_1	n	p-value
Base	−0.9663	250,041,611	−932,653	15	2.41E-09
Unnotched	−0.9440	195,279,275	−865,535	8	2.11E-04
1 mm Slide	−0.9801	205,580,722	−924,405	8	9.76E-06
Common	−0.9604	202,382,557	−911,104	31	1.22E-17

some variation in the difference between them.

3.1 Linear regression

The first three rows of Table 3 summarise the results for each model family when 95th percentile Von Mises stress (in MPa) is regressed on angle (in degrees).

For each family, the observed linear correlation coefficients r and associated p-values indicate significant negative linear association between 95th percentile Von Mises stress and angle. Values of the estimated regression coefficients b_0 and b_1 are significantly different from zero for all families, meaning that linear prediction equations of the form $\hat{y} = b_0 + b_1 x$, where $\hat{y}$ is the predicted 95th percentile Von Mises stress and x is the angle, are reasonable for each family. These equations are represented graphically in Figure 4.

The regression lines for the different families of models are shown in Figure 4. Consistent with the data points, the regression lines imply that the un-notched family of models has, for a given angle, a lower maximum stress than the base family of models. This indicates that the base (notched) family of models experiences a greater degree of stress concentration due to the notch, above and beyond what is experienced by removing the rounded edges on the compression plate.

However, the apparent differences between the regression lines are not

statistically significant. When tested for collinearity, the hypothesis that the linear relationship between stress and angle is the same for all three families is retained (p-value is 0.5589). Therefore it is sensible to combine all data points and determine a common linear regression equation, which is summarised in the fourth row of Table 3 and expressed in rounded values as

> Predicted 95th percentile Von Mises stress $= 200 \times 10^6 - 910 \times 10^3 \times x$, where x is the angle in degrees.

The common regression equation indicates that 95th percentile stress reduces by about one third over the range of angles used in the modelling. That is, as the angle is increased by $35°$ (from $115°$ to $150°$) there is a lessening of the stress experienced by the DHS in the order of 33%. The regression equation can only reasonably be applied for angles between $115°$ and $150°$. According to the findings of Nissen et al. [8], it is likely that female NOF angles will lie well within this range. A potential use for this relation is that surgical staff might opt for a DHS with an angle greater than that of the NOF in the patient, provided there is enough room for it in the bone, in an effort to reduce the maximum stress experienced by the DHS in situ.

After performing FEA, the values of Von Mises stress are collated for each node and the 95th percentile of the maximum stress is obtained. Using regression, the formula $\hat{y} = 200 \times 10^6 - 910 \times 10^3 \times x$ is derived relating predicted 95th percentile Von Mises stress ($\hat{y}$, MPa) to angle (x, degrees) over the range $115°$ to $150°$ for a generic DHS. It comes from a very generic case of DHS, where information for its geometry has been obtained from Stryker [10] and Synthes [11].

4 Conclusion

The notch that develops in models with rounded edges and a compression plate angle of less than 135° is a greater stress concentrator than leaving the edges of the plate sharp. However, these differences are minimal. Modelling shows a 33% drop in stress from the smallest to the largest compression plate angle. This implies that surgical staff may be able to give a DHS with an angle greater than that of the patient's NOF, provided there is room within the bone itself, to lower the maximum stress generated.

Acknowledgements The authors thank Miss Aspriha Chakraborty for her help in preparation of the manuscript.

References

[1] Cosmosworks, Structural research and analysis corporation, Santa Monica, USA, 2007. [2 Oct 2008] http://www.cosmosm.com. C225

[2] Edwards, T. R., Tevelen, G., English, H. and Crawford, R., Stripping torque as a predictor of successful internal fracture fixation, *ANZ J. Surg.*, **75**, 2005, 1096–1099. C224

[3] Hip fracture, Wikimedia Commons, [5 Aug 2008] http://commons.wikimedia.org/wiki/Hip_fracture. C221

[4] Johansson, T., Bachrach-Lindstrom, M., Aspenberg, P., Jonsson, D. and Wahlström, O., The total costs of a displaced femoral neck fracture: comparison of internal fixation and total hip replacement, *International Orthopaedics*, **30**, 2006, 1–6. doi:10.1007/s00264-005-0037-z C221

[5] Kemler, M. A., de Vries, M., Gerard, W. J., van Raay, J. J. A. and Van der Tol, A., Can we predict failure of internal fixation when treating femoral neck fractures? *Eur. J Orthop. Surg. Traumatolo.*, **17**, 2007, 67–70. C224

[6] Marieb, E. N. Human anatomy and physiology, 6th ed., Pearson Benjamin Cummings, San Francisco, 2004. C221

[7] Medicare Benefits Schedule (MBS) Item Statistics Reports 2007, Medicare Australia, [31 May 2007] http://www.medicareaustralia.gov.au/statistics/dyn_mbs/forms/mbs_tab4.shtml C224

[8] Nissen, N., Hauge, E. M., Abrahamsen, B., Jensen, J. E., Mosekilde, L. and Brixen, K., Geometry of the proximal femur in relation to age and sex: a cross-sectional study in healthy adult Danes, *Acta Radiologica*, **46**, 2005, 514–518. doi:10.1080/02841850510021562 C224, C226, C227, C228, C233

[9] Solidworks, SolidWorks Corporation, Concord, Mass, 2007, [2 Oct 2008] www.solidworks.com. C225

[10] Stryker, Omega3 compression hip screw system, [5 August,2008] http://www.stryker.com/en-us/products/Trauma/HipFracture/Omega3CHS/index.htm C224, C226, C227, C233

[11] Synthes, North America, DHS/DHS Dynamic hip and condylar screw system: Technique Guide 1990, [26 October 2007] http://products.synthes.com/prod_support/Product%20Support%20Materials/Technique%20Guides/SUSA/SUTGDHS-DCSJ3045B.pdf. C226, C227, C233

[12] Weinrauch, P. Intra-operative error during Austin Moore hemiarthroplasty, *J. Orthopaedic Surgery*, **14**, 2006, 249–252. C221

Author addresses

1. **John Arundell**, Faculty of Engineering and Industrial Sciences, Swinburne University of Technology, Hawthorn, Melbourne, Australia.

2. **Aaron Blicblau**, Faculty of Engineering and Industrial Sciences, Swinburne University of Technology, Hawthorn, Melbourne, Australia.

3. **David Richards**, Faculty of Engineering and Industrial Sciences, Swinburne University of Technology, Hawthorn, Melbourne, Australia.

4. **Manmohan Singh**, Faculty of Engineering and Industrial Sciences, Swinburne University of Technology, Hawthorn, Melbourne, Australia.
   mailto:msingh@swin.edu.au